Reports

Light Scattering by Irregular Randomly Oriented Particles

Abstract. *A method for calculating light scattering by irregular randomly oriented particles yields results that are in good agreement with experimental data. The method is based on the assumption that surface waves are present in scattering by spherical particles, but they are absent in scattering by irregular particles.*

The scattering of light by small particles is a phenomenon of considerable importance in several fields of science, such as astronomy, atmospheric science, and chemistry, to name just a few. In many practical problems it is assumed that the small particles (cosmic dust particles, atmospheric aerosols, and macromolecules) are spherical.

Sphericity is assumed because the scattering problem can be solved theoretically only for a very few highly symmetric shapes, such as spheres, spheroids, or infinitely long cylinders. For all other shapes one must solve the Maxwell equations numerically for boundary conditions determined by the shape of the scattering particle. For a wide range of possible size distributions, shapes, and orientations of an ensemble of nonspherical particles, such calculations cannot be performed without an excessive demand on computer time. Even if the numerical solution for each individual nonspherical particle could be obtained, many details of the scattering angular pattern (the so-called phase function) would be lost during the processes of averaging over all possible particle orientations, summing over all possible shapes, and integrating over the distribution of particle sizes. The resulting phase function for an ensemble of irregular randomly oriented particles would be a very smooth curve characterizing only some basic differences between the scattering by spherical and that by nonspherical particles (*1*). As an alternative, we are proposing an approximation which gives only a basic modification for nonsphericity without going into details of the solution of the Maxwell equations for each individual nonspherical particle.

The first problem is to establish the existence of a unique feature characteristic of scattering by spherical particles but not present when the scattering occurs on randomly oriented particles of other shapes. A well-known feature satisfying this requirement is the glory (*2*), a strong enhancement of scattering in the backward direction.

The glory is caused by surface waves (*3*); the same surface waves are responsible for the ripple structure in the normalized extinction cross section (*4*). It has been shown (*4*) that in the range of refractive indices $m \leq 2$ and of size parameters $x \leq 30$ there is a one-to-one correspondence between the surface waves and resonances in the Mie amplitudes a_n and b_n occurring around the size parameter $x \sim n$. The size parameter $x = 2\pi r/\lambda$ relates the sphere radius r to the wavelength λ of the scattered radiation. Definitions of a_n and b_n can be found in (*3*). The integer n is the summation index used in the Mie partial wave series.

To illustrate what we mean by resonances, Fig. 1 shows real (Re) and imaginary (Im) parts of a_{10} and b_{10} as a function of x for $m = 1.50$. The sharp peaks observed at $x \sim 9$, for which $\mathrm{Re}(a_n)$ and $\mathrm{Re}(b_n)$ reach a maximum value of one, are called resonances. It is these resonances that cause the glory and the ripple structure in the Mie calculations for spherical particles (*4*).

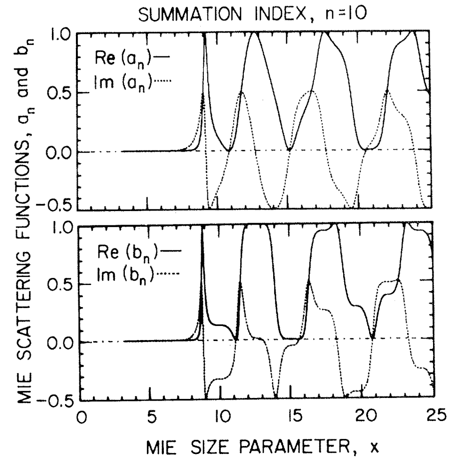

Fig. 1. Resonances in Mie scattering functions a_n and b_n. These curves refer to Mie calculations for refractive index $m = 1.5$ and for summation index $n = 10$; the sharp peaks in the curves for $x \lesssim 10$ are resonances.

We conjecture that such resonances cannot exist if the scattering particles have shapes drastically different from highly symmetrical shapes such as spheres. Consequently, we propose that the first-order correction for nonsphericity of scattering particles should be the removal of partial wave resonances from the Mie calculation (*4*).

Our conjecture leads to a simple scheme for computing the scattering on nonspherical particles. We use the Mie theory, with the exception that the scattering functions a_n and b_n in resonance regions—for example, near the first peak in $\mathrm{Re}(a_{10})$ and $\mathrm{Re}(b_{10})$ in Fig. 1—must be modified.

Each amplitude a_n and b_n can be written in the form (*5*)

$$a_n(x,m) = \tfrac{1}{2}[1 - S_a{}^n(x,m)]$$

and

$$b_n(x,m) = \tfrac{1}{2}[1 - S_b{}^n(x,m)]$$

The first term on the right-hand side of these equations represents diffraction. The second term on the right, denoted by $S_a{}^n$ or $S_b{}^n$, is a function of the refractive index, size, and shape of the scattering particle; this term is responsible for the partial wave resonances in a_n and b_n. Consequently, for scattering by nonspherical particles we set $S_a{}^n(x,m)$ or $S_b{}^n(x,m)$ equal to zero in the resonance region.

Practically, this means that we set $a_n = \tfrac{1}{2}$ or $b_n = \tfrac{1}{2}$ whenever $\mathrm{Re}(a_n)$ or $\mathrm{Re}(b_n)$ is in a resonance region. There is a single restriction on the above procedure: the surface wave on a spherical particle can exist only if the size of the sphere is larger than the wavelength of the incident radiation. Our study of the Mie amplitude functions shows that the concept of a resonance in a_n or b_n breaks down at small values of x. For this reason, the modifications should not be applied to all a_n and b_n functions starting with the summation index $n = 1$; instead, they should be applied only to a_n and b_n values between some index $n = n_1$ and the largest value of n used in the ordinary Mie calculations.

We carried out a series of experimental studies to help us establish the best

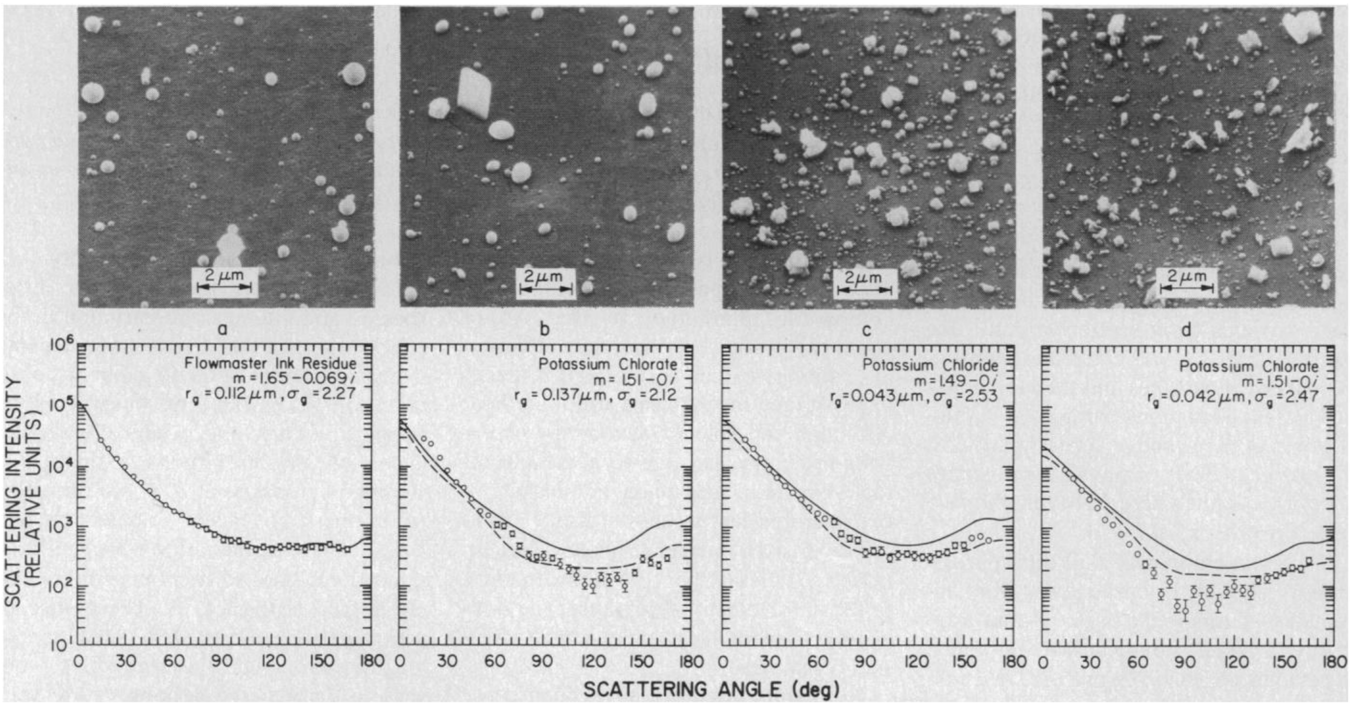

Fig. 2. Comparison of measured angular scattering patterns at $\lambda = 0.6328$ μm (circles with error bars) with those calculated by Mie theory (solid lines) and the modified Mie theory with $n_1 = 3$ (dashed lines). Particle composition and complex refractive index are identified on each scattering diagram; each diagram also contains the geometric mean radius r_g and geometric standard deviation σ_g for log-normal size distributions (7) obtained by determining the radii of spheres of equal cross sections for several thousand particles from scanning electron microscope photographs. Examples of such photographs are presented above the scattering diagrams to illustrate their respective particle shapes.

value of n_1 to be used in our modified Mie calculations. We generated, under controlled laboratory conditions, aerosol particles with known refractive index, and with sizes comparable to those normally observed in the earth's atmosphere. We measured scattering phase functions for various types of particles with a polar nephelometer (6). We documented particle shapes and size distributions by means of scanning electron microscope photographs of particles collected onto Nuclepore filters. Using the known data on refractive index and particle size distribution, we then compared these experimental results with results obtained by Mie calculations and with results obtained from our approximation.

Figure 2 illustrates the major results of our intercomparisons between measured and calculated phase functions. We obtained almost exact agreement between experimental data and the Mie calculations for the case of spherical particles, as shown in Fig. 2a. For nonspherical particles, we obtained best agreement between measurements and calculations using the modified Mie theory with $n_1 = 3$; this is equivalent to the assumption that the surface wave on a sphere can exist only for size parameters $x \gtrsim 3$. For comparison, the size of irregular particles used in our experimental measurements is in the range between $x = 0.4$ and $x = 18$. The results of this correction are shown in Fig. 2, b to d. It was often not possible to get close fits between the measured and calculated angular scattering patterns when the distribution of particle shapes included an appreciable fraction of particles with one dimension longer than the others, as illustrated by the ellipsoids in Fig. 2b and the irregular particles in Fig. 2d. We suspect that such an aerosol may result in preferentially oriented particles, thereby violating the assumption of random particle orientations.

If we modified the Mie functions a_n and b_n for all summation indices $n \geq 1$ (rather than $n \geq 3$), we would subtract more from the scattering amplitudes than the typical effect of nonsphericity; that is, we would overestimate the influence of the particles' nonspherical shape on

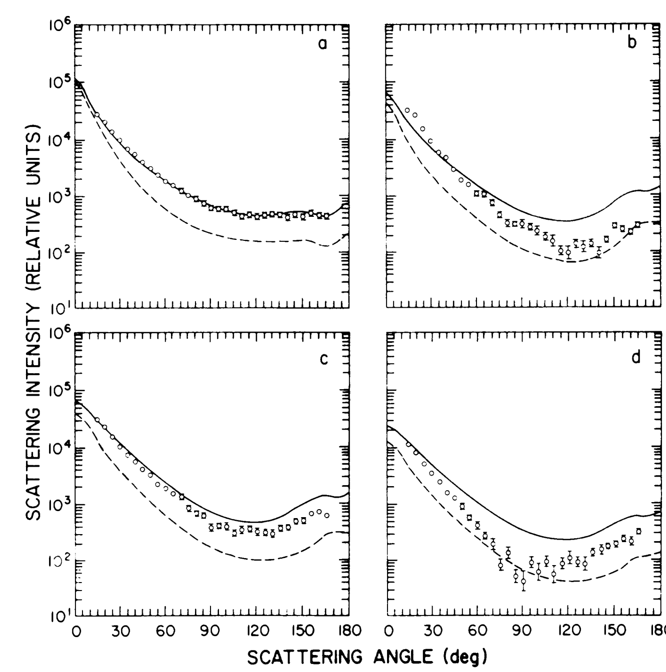

Fig. 3. Comparison of measured angular scattering patterns with those calculated by Mie theory (solid lines) and our limiting approximation with $n_1 = 1$ (dashed line) for the cases shown in Fig. 2.

scattering. In this case we would not necessarily expect to get very good agreement between calculations and experimental results, but those calculations could be used as an upper limit for the effect of nonsphericity on scattering characteristics of interest. The result of such calculations, as shown in Fig. 3, can be useful in many applications. For example, in deducing the physical properties of atmospheric aerosols or cosmic dust particles from scattering data, one can use first the Mie calculation assuming spherical particles and then the modified Mie calculations with $n_1 = 1$. Regardless of the shape of aerosol particles, the correct values of physical properties should be somewhere between the two sets of results, as in Fig. 3.

We again emphasize that our approximation should be used only for ensembles of randomly oriented and arbitrarily shaped nonspherical particles. Whenever all particles are oriented in a definite direction or whenever the scattering occurs on a single particle, specific effects depend on a particle's exact shape; since these effects are not included in our approximation, it should not be used. In addition, our intercomparisons were made for particles in the Mie size range $x < 30$. This adequately covers the size range, for example, of the normal background aerosol particles in the earth's atmosphere; further studies will be required before the procedure can be applied to larger sizes.

PETR CHÝLEK
Department of Geosciences, Purdue University, West Lafayette, Indiana 47907, and
National Center for Atmospheric Research, Boulder, Colorado 80303
G. W. GRAMS
National Center for Atmospheric Research
R. G. PINNICK
Atmospheric Sciences Laboratory, U.S. Army Electronics Command, White Sands Missile Range, New Mexico 88002

References and Notes

1. A. C. Holland and J. S. Draper, *Appl. Opt.* **6**, 511 (1967); A. C. Holland and J. Gagne, *ibid.* **9**, 1113 (1970).
2. J. E. Hansen and L. D. Travis, *Space Sci. Rev.* **16**, 527 (1974).
3. H. C. van de Hulst, *Light Scattering by Small Particles* (Wiley, New York, 1957), chap. 17.
4. P. Chýlek, *J. Opt. Soc. Am.* **66**, 285 (1976).
5. ——, *ibid.* **65**, 1316 (1975).
6. G. W. Grams, A. J. Dascher, C. M. Wyman, *Opt. Eng.* **14**, 80 (1975).
7. G. Herdan, *Small Particle Statistics* (Butterworths, London, 1960), chap. 6.
8. The National Center for Atmospheric Research is sponsored by the National Science Foundation. P.C. was partially supported by a grant from the Atmospheric Science Section of the National Science Foundation.

31 March 1976; revised 2 June 1976

Hooked Trichomes: A Physical Plant Barrier to a Major Agricultural Pest

Abstract. *Hooked epidermal appendages (trichomes) on leaves of field bean cultivars effectively capture nymph and adult leafhoppers. Frequency of capture and capture mortality are highly correlated with trichome density. Hooked trichomes inserted at angles less than 30° are ineffective in capture.*

Breeding crop plants for genetic resistance to insect pests is an ecologically compatible alternative to the use of chemical pesticides. Selection of resistant cultivars can be accelerated if specific resistance mechanisms are identified. Although the role of secondary chemicals in plant resistance to herbivore attack has received much emphasis (*1*), considerably less is known about physical defensive barriers in plants. Recent review articles (*2*) have brought attention to the involvement of glandular and nonglandular plant hairs (trichomes) in insect resistance.

Numerous attempts have been made to establish a statistical correlation between the degree of crop pubescence and resistance to leafhoppers of the genus *Empoasca* (Walsh) (*3*), major worldwide pests of cotton, soybeans, alfalfa, clover, field beans, and potatoes. In North America *Empoasca fabae* (Harris), the potato leafhopper, is a serious pest of field beans, *Phaseolus vulgaris* L. In South America and Central America a closely related species, *Empoasca kraemeri* Ross and Moore, is a primary limiting factor in the production of this vital protein crop (*4*). Although there have been anecdotal reports of arthropod capture by hooked trichomes of *P. vulgaris* (*5–7*), the specific impact of pubescence in different cultivars of field beans on the population biology of leafhopper pests does not appear to have been determined (*8*). In this report, we describe a direct relationship between the hooked trichomes of *P. vulgaris* and mortality of *E. fabae* and report the basis for intraspecific and interspecific variation in the effectiveness of this defense mechanism.

During studies of feeding damage of *E. fabae* on field beans, we observed leafhopper nymphs and adults clinging to leaves of certain cultivars. Using a dissecting microscope at 60×, we observed leafhoppers physically impaled on leaf hairs. Closer examination revealed large numbers of hooked trichomes on the undersurface of the leaves. These specialized hairs ranged from 0.06 to 0.11 mm in length; hairs over the leaf veins were slightly longer. As leafhoppers are very active, we concluded that the insects had become entangled in the hairs as they moved rapidly over the leaf surface.

To document the various methods of capture, we examined captured leafhoppers on bean leaves by scanning electron microscopy (*9*). Both nymphs and adults were found to be impaled through the intersegmental membranes of the abdomen by hooked trichomes (Fig. 1, a and b), to our knowledge a previously unreported phenomenon. Insects were also captured by trichomes impaled in the tarsal segment of the leg or entangled in the tarsal claws, as reported for other insect species (*6, 7*). Figure 1c illustrates yet another form of capture, by a trichome embedded in the membrane between the tibia and the tarsus.

Leafhoppers captured by the tarsus or tibia terminate feeding and struggle to free themselves from the trichomes, fre-

Table 1. Relationship between density of hooked trichomes and capture mortality of leafhopper nymphs caged on leaves of field beans and lima beans. Means followed by the same letter within a column are not significantly different at $P = .05$ by Duncan's multiple range test.

Cultivar	Node	Leaf surface	Hooked trichome density (No. per cm²)	Capture (%)	Capture mortality (%)
Phaseolus vulgaris	Terminal	Lower	14,241 a	59.8 a	36.8 a
'California Light	4	Lower	1,955 b	50.0 b	31.5 ab
Red Kidney'	2	Lower	1,593 b	36.4 c	26.8 b
	2	Upper	244 e	5.7 ef	2.6 d
Phaseolus vulgaris	4	Lower	435 d	16.9 d	12.4 c
'Brasil 343'	2	Lower	362 de	13.2 de	7.6 cd
	2	Upper	11 f	0.5 f	0.0 d
Phaseolus lunatus 'Henderson Bush Lima'	2	Lower	841 c	4.5 ef	2.0 d